Predictions for Modern Jet Quenching Observables at RHIC Energies with JEWEL 2.2.0

Ahmed Alenezi

Department of Physics
University of Colorado, Boulder

Defense Date: March 18, 2021

Thesis Advisor

Prof. Dennis Perepelitsa - Department of Physics

Thesis Committee Members

Prof. John Cumalat - Department of Physics

Prof. Dennis Perepelitsa - Department of Physics

Dr. Divya Vernerey - Department of Mathematics

ABSTRACT

When highly relativistic beams of nuclei are brought into collision, they create a Quark Gluon Plasma (QGP), a hot and exotic state of matter that also existed just after the Big Bang. By studying it, we can learn about the strong nuclear force and about the conditions of the Early Universe. In 2023, the Relativistic Heavy Ion Collider will begin to deliver high-statistics gold-gold (Au+Au) collision data to the new sPHENIX and existing STAR detectors. New experimental capabilities at these detectors will allow for a better understanding of how hard scattered partons propagate and lose energy in the quark-gluon plasma. Here, we use the latest version of JEWEL to study jet quenching observables which can be measured for the first time at RHIC. JEWEL is a Monte Carlo event generator that simulates jet evolution in a perturbative framework in both proton-proton and nucleus-nucleus collisions and has been mostly used for making predictions at LHC energies. JEWEL studies at RHIC energies may help guide the physics program and analysis techniques in the mid-2020's. In particular, JEWEL now includes photon-jet processes which are important to the sPHENIX physics program, as well as an improved medium response. I present results for jet quenching observables which can be measured with high-statistics Au+Au data-taking at RHIC 2023.

CONTENTS

ACKNOWLEDGEMENTS

I would like to thank my advisor Dennis Perepelitsa. I am grateful for his constant help and guidance. I sincerely appreciate all his efforts to help me with my research despite the difficult circumstances. His passion and enthusiasm made my experience working with him invaluable.

I would also like to thank everyone in the Heavy-Ion group for everything that I learned from them. I am grateful for being in a group that has such a positive and supportive environment. Special thanks to Jeff Ouellette who was helping me on my project from the moment I joined the group.

I am deeply grateful for all the love and support that I had from my friends and family who constantly supported me despite the long distance and time difference. I am thankful for everything they did to help me succeed.

I. INTRODUCTION

The field of heavy ion physics has made a great progress in telling us the story of the first moments of the universe 13.8 billion years ago (preceded only by the electroweak phase transition). It is now known that for a very short time after the Big Bang, the entire universe was in a state with extremely high temperature and density conditions. Physicists managed to generate similar conditions in the lab by colliding energetic beams that travel at highly relativistic speeds and create what we call the Quark-Gluon Plasma (QGP). The largest labs that study this physics are the Large Hadron Collider (LHC) and the Relativistic Heavy Ion Collider (RHIC). To compare data to theory, many theoretical models are used to study different aspects of the physics contained in the data. One popular model is called Jet Evolution With Energy Loss (JEWEL) [1]. JEWEL has been used extensively to study the physics at both RHIC and LHC. A new release of JEWEL (JEWEL 2.2.0) was published with the addition of a new perspective on how the QGP medium interacts with the produced hard partons (i.e., partons with large transverse momentum) [2].

However, since the publication of JEWEL 2.2.0, physicists are excited to use these updates in JEWEL to study various aspects of energy loss. In addition, the new upgrades in the sPHENIX and STAR detectors at RHIC can be thoroughly studied with the new tools JEWEL 2.2.0 provides [3].

New studies are needed to understand the physics at RHIC and make predictions for the data that will be delivered in the early 2020's. The aim of this thesis is to use JEWEL 2.2.0 to make predictions for the physics at RHIC. As a probe for studying the QGP medium, I will work with jet quenching observables and test them in JEWEL 2.2.0.

A. The Physics at RHIC

RHIC is one of the largest particle colliders in the world and is located at Brookhaven National Laboratory (BNL) in New York. The main goal of the RHIC experiment is to study the outcomes of the collisions that take place at one of its detectors. We start the experiment by injecting two beams of charged particles inside the accelerator. The accelerator moves the beams in a circular path using an alternating electric field for linear acceleration and a magnetic field to keep the beams in circular motion. The two beams are kept separated and travel in opposite directions. When the two beams reach high energies (their speeds will be very close to the speed of light), we focus the beams inside a detector where they collide [4]. There are many collision systems that one can study to understand different physics. For the purpose of this thesis, we will only focus on two systems; proton-proton collisions and heavy-ion collisions (ions with atomic mass larger than Helium).

To understand the physics of the collisions, we use the standard model as a theoretical framework that explains the three fundamental forces: the electromagnetic force, the strong force and the weak force. Each force has its own force carrier (or mediator) that causes the interaction between particles (Fig. 1). Those mediators are: photons (electromagnetic force), gluons (strong force) and the $W^{\pm}$ and Z^0 bosons (weak force). For our purposes, the weak force is negligible. Similar to the role of charge in the electromagnetic force, the strong force is sourced by the presence of color. Partons (quarks and gluons) are the only particles that carry color and hence they are the only ones that interact strongly. Even though quarks are charged, the most dominant force in the interaction between quarks is the strong interaction in short distances. As we mostly work with quarks in heavy ion physics, the most relevant force is the strong force carried by gluons. The theory that governs the strong interaction is called Quantum Chromo-Dynamics (QCD). For all intents and purposes, when working on heavy ion physics, we are practically working with QCD.

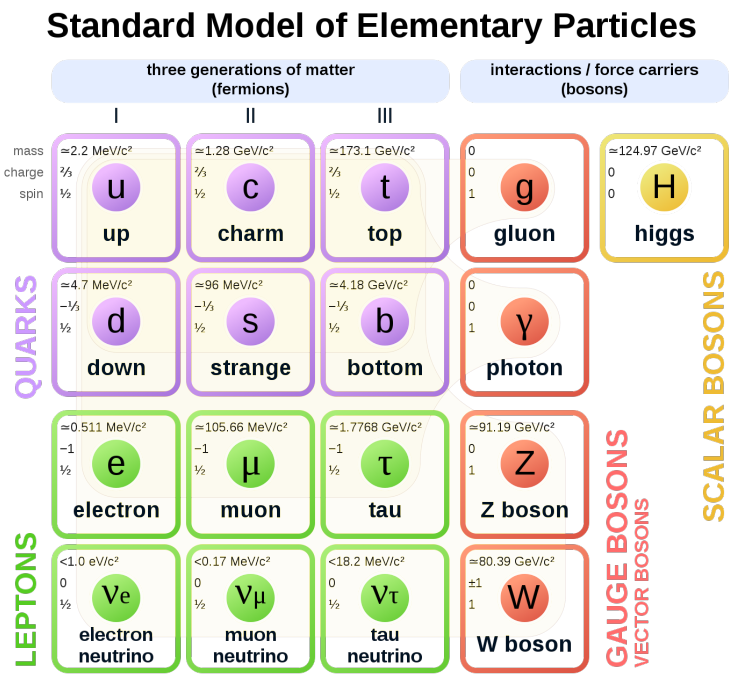

FIG. 1. Matter particles and force mediators in the standard model. Figure from [5].

B. Coordinate System

When the two beams collide, we use a coordinate system that was specifically defined to work with the physics at detectors [4]. First, we define the axis of the collision as the z-axis. Also, we define the transverse plane as the plane that is perpendicularly intersected by the z-axis (which is a fancy name for the xy-plane). Now, there are three important parameters that are necessary to understand:

- **Phi** (ϕ): The angle from the x-axis in the xy-plane.
- **Pseudorapidity** (η): A parameter associated with the angle θ between a particle and the transverse plane. It is defined as:

$$\eta = -\ln\left(\tan\left(\frac{\theta}{2}\right)\right)$$

  Pseudorapidity is conventionally used instead of the explicit θ angle.

- **Transverse Momentum** (p_T): The projection of a particle's momentum onto the transverse plane. Or simply, $p_T = \sqrt{p_x^2 + p_y^2}$

Whenever found, ΔR between two objects A and B is defined as:

$$\Delta R = \sqrt{(\eta_A - \eta_B)^2 + (\phi_A - \phi_B)^2}$$

C. p+p Collisions

The first of the two systems that we study is proton-proton (p+p) collisions. Inside each proton, there are three quarks (uud). When the two proton beams collide, we get parton-parton scatterings. Hard processes produce new high p_T partons (or possibly vector bosons) following Feynman rules. Two possible processes that we will study here are: di-jet and γ-jet processes. In di-jet processes, the product of a parton-parton scattering is another pair of partons, and in the case of RHIC energies, the partons are more likely going to be a pair of a quark and an anti-quark ($q\bar{q}$). Due to conservation of momentum, the pair starts with the same initial p_T with opposite directions in the COM frame. Due to the non-perturbative behavior of QCD at long distances, the potential between the two quarks is linear (unlike QED where the potential is proportional to $1/r$) [6]. Because of color confinement, it is practically impossible to detect isolated partons. Billions of events observed at the LHC and RHIC confirm this impossibility. When the distance between the two quarks increases, it becomes energetically favourable to convert part of the energy into new massive pairs of partons. The production of massive particles stabilizes the system [7]. This process repeats itself until the partons lose enough energy to form bound states of mesons and baryons. This process is called "*Hadronization*".

In the process of hadronization, there are two limits that govern how the splitting of partons happens: the collinear limit and the soft limit [4]. Both limits come from the conservation of transverse momentum. Suppose that a quark radiates a gluon. The two limits then become as follows:

- **Collinear Limit**: The angle between the gluon and the quark goes to zero. At the COM frame, the quark and gluon will each carry half the p_T of the initial quark.

- **Soft Limit** : The angle between the gluon and a quark goes to $\frac{\pi}{2}$, where the quark continues in its initial path and the gluon is perpendicular to it. Now, the energy shared by the gluon goes to zero, and the quark takes all the initial p_T.

Even though soft (low p_T) radiations are far more common, they do not affect the energy of the the hard partons. Therefore, most energetic partons will be concentrated around the path of the hard parton. In detectors, we see this as energetic hadrons are deposited in a relatively small radius in the η-ϕ plane. We call those sprays of hadrons "*jets*". Jets give us access to the initial energy of the hard partons in the event.

This description of jets is only qualitative. Quantitatively, it is more complicated to construct jets due to the ambiguity of the definition both theoretically and experimentally. There are many algorithms used to construct jets from final states hadrons. By far, the most used jet clustering algorithm that captures hard particles is called *"anti-k_T"* [8]. To perform anti-k_T, we follow those steps [9]:

1. For any two particles i and j we find:

$$d_{ij} = min(\frac{1}{p_{T,i}^2}, \frac{1}{p_{T,j}^2})\Delta R_{ij}^2$$

$$d_{iB} = \frac{R^2}{p_{T,i}}$$

   Where R is the cone size of the jet (a free parameter).

2. If $d_{ij} > d_{iB}$, then we combine the two particles into a new object that has the p_T-weighted average of the positions. We perform this step again with the new object treated as a particle.

3. If $d_{ij} < d_{iB}$, then we stop iterating, and label i as a jet.

This method makes sure that neighboring particles are combined, and particles far from the jet axis are excluded. Also, soft particles will have little effect on the jet as they are absorbed by hard particles. This scheme-like algorithm is going to play an important role when discussing jet sub-structure in chapter IV.

D. Heavy-Ion Collisions

As interesting as they can be, p+p collisions are only used as a reference when we study QGP. The main focus of study in heavy-ion physics is the production of QGP in heavy-ion collisions. When two ions collide, they overlap with some centrality (with 0% centrality being full overlap (central) and 100% centrality being no overlap at all (peripheral)). The parts of the ions outside this overlap are called *"spectators"* and they do not contribute to the physics studied as they continue moving in the beam axis direction and cannot be detected in cylindrical detectors. Partons inside the nucleons in the overlap area experience two extreme conditions [10]:

- **High temperature**: The temperature of the overlap area could reach 360 MeV at RHIC, which is about 250K times hotter than the center of the sun. This temperature increases the energy of the partons, and liberates them from their bound states (protons and neutrons).

- **Large baryon density** : The number density of the baryons in the overlap area is very large. The problem with this is that Pauli's exclusion principle does not allow any two particles to occupy the same quantum state. With that large density, we are pushing the limits of Pauli's exclusion principle with those extremely energetic baryons, and one way to get over it is to liberate the partons and create more quantum states.

In high energy heavy-ion physics, we are interested in the high temperature limit. First, due to relativistic length contraction, the ions look like disks. The strong force causes those disk-like ions to have a large pressure from outside towards the center of the overlap area. After the collision, the high temperature breaks the nucleons from the ions and the quarks from the nucleons. Now, we have a liquid-like medium that contains strongly interacting *"de-confined"* partons. The de-confined state has a very small viscosity that can by studied using the laws of hydrodynamics of a perfect liquid. This medium is what we call Quark-Gluon Plasma.

Because of the strong force, hadrons (mostly pions) start to form immediately after the collision. It only takes $10^{-23}s$ for the QGP phase to start and end. Working with this extremely short period of time is a real challenge for physicists. We also have little control over the particular details of any given collision. To overcome those difficulties, physicists

use different probes to get as much information as possible. The probe that will be used in this thesis is called *"jet quenching"*, which is the topic of chapter III.

II. JEWEL 2.2.0

Jet Evolution With Energy Loss "**JEWEL**" is a Monte Carlo event generator that simulates jet evolution in a perturbative framework in both proton-proton and nucleus-nucleus collisions [2]. JEWEL studies the interaction between jets and the Quark-Gluon medium in ion-ion collisions, and it has been successful in describing different aspects of jet quenching observed in data. Some general features of JEWEL that are worth mentioning are:

- In proton-proton events, JEWEL does not include Underlying Event (UE).
- In ion-ion events, JEWEL does not include remaining events.
- In JEWEL, the centrality of the ion-ion collision is specified by the user

JEWEL has been widely used to study heavy ion physics at both LHC and RHIC energies. In 2014, a new version of JEWEL was published and made available for the public [11]. The new release of JEWEL treats the medium as a collection of thermal partons that interact with the constituents of jets. This interaction causes recoiling partons to carry away part of the jets' energy through re-scattering. However, those recoiling partons thermalize only partially in the medium and the medium responds to this partial thermalization by adding a soft particle contribution in the jet cone. Part of this soft background is correlated with the jet and we need to keep it as this is in fact part of the energy of the jet. However, those soft contributions have a thermal component to them that needs to be subtracted before working with observables as would be measured in data.

JEWEL is one of a few models that modify the dynamics of the evolution of jets in the medium. Other models assume that jet evolution is unmodified in the medium, and jet quenching effects are added separately depending on medium properties. One difference this has on the observable physics is that, unlike other models, jet quenching in JEWEL does not primarily come from path length. Instead, it relies heavily on the energy loss fluctuations [12]. We see this in its projections for the di-jet asymmetry and in the path-length dependence of jet modification, which will be explored later in the thesis.

A. Subtraction Methods

In a paper published in 2017, the authors of JEWEL proposed two methods to subtract thermal contributions from soft interactions to jet energies [13]. Before working with observables sensitive to the energy of particles in the event such as in jet quenching, we need to use one of those methods. The two proposed subtraction methods are:

1. 4-Momentum Subtraction

4MomSub is a jet level subtraction method. That is, when subtracting, only the total kinematics matter. Particles are only needed when we cluster jets at the beginning to get the total energy. Instead, we use objects called *"thermal momenta"* to subtract energy directly from jets (Fig. 2). When subtracting using the 4MomSub method, we perform the following steps:

1. Using the anti-k$_T$ algorithm, we cluster jets from real particles (status 1).

2. We go over each jet and look for all thermal momenta within it. After we identify all thermal momenta that are within $\Delta R = 10^{-5}$ of any dummy particle inside the jet, we subtract the thermal momenta from the jet's 4-momentum. That is:

$$p^{\mu}_{new\ jet} = p^{\mu}_{old\ jet} - \sum p^{\mu}_{thermal\ momenta}$$

3. The collection of subtracted thermal momenta is the thermal background in each jet.

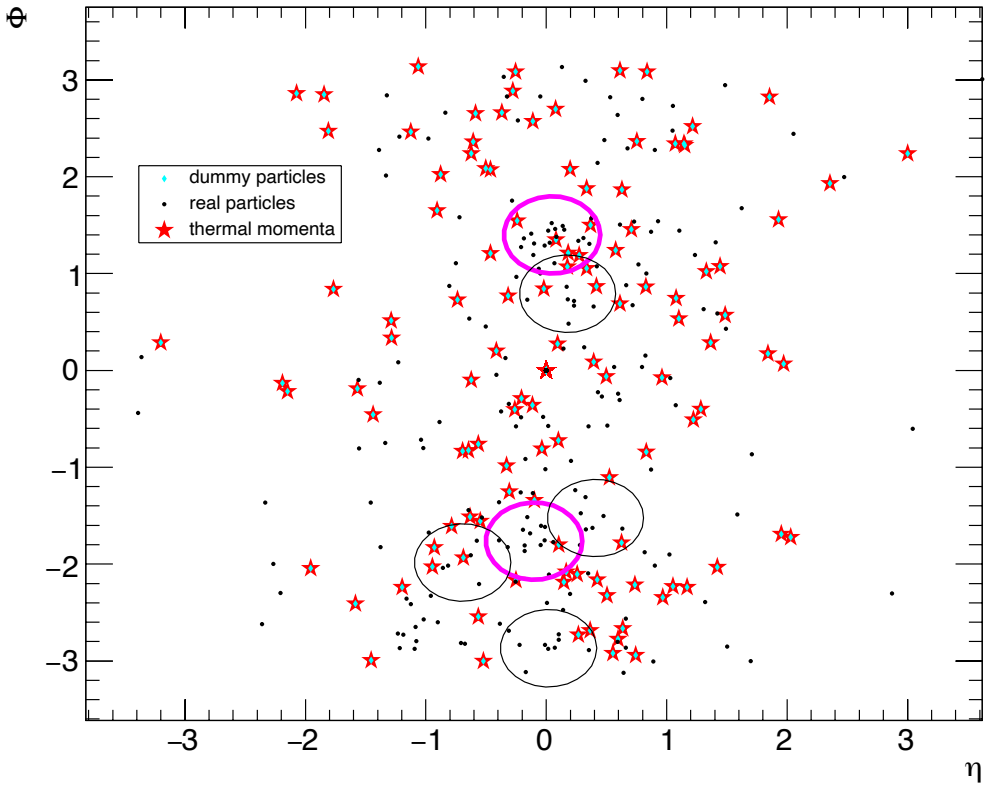

FIG. 2. A scatter plot for a medium event in JEWEL 2.2.0. The ellipses are anti-k$_T$ jets with cone size $R = 0.4$. The purple ellipses are the most energetic jets in the event. The scatter plot shows a random event layout of dummy particles (blue), real particles (black) and thermal momenta (red). We subtract the thermal momenta from a jet's 4-momentum for all thermal momenta that lie inside the jet cone (i.e. the ellipse).

2. Grid Subtraction

GridSub is actually divided into two methods (GridSub1 and GridSub2). This is because we can perform subtraction after or before clustering the jets. Here, I only investigate GridSub2 as it is computationally more convenient to work with, particularly when working on jet sub-structure. GridSub2 is a constituent-level method. That is, we use the information about the individual particles in the event to perform the subtraction. When subtracting using the GridSub2 method, we perform the following steps:

1. Place a grid with some resolution over the η-ϕ plane (Fig. 3). We chose 0.1×0.1 cell size for the grid.

2. Assign a 4-momentum vector to each cell using:

$$p^{\mu}_{cell} = \sum p^{\mu}_{final\ state\ particles} - \sum p^{\mu}_{thermal\ momenta}$$

   where the summation is over particles in the cell

3. Disregard cells with $p_T < 0$ by setting $p^{\mu}_{cell} = 0$

4. Use anti-k_T to cluster jets using subtracted cells as inputs.

Each method can be useful when we study jets. For example, unlike the GridSub2 method, which removes thermal contributions only partially, 4MomSub removes all thermal contributions, hence results in a more accurate jet energy. However, for computational reasons, GridSub2 is more convenient to use for jet substructure. 4MomSub (and GridSub1) methods are "subtracting after clustering" methods, whereas GridSub2 is a "clustering after subtracting" method. The reason why this is relevant for jet substructure is that for GridSub2 we get a "fastjet::pseudojet" object after we finish the subtraction, which can be used as an input to the SoftDrop package to study jet substructure. On the other hand, 4MomSub (and GridSub1) give us a vector object when we finish subtraction with no clustering history, which means that we cannot directly use them in SoftDrop (As an alternative, we could cluster jets without subtraction and use SoftDrop to find subjets. Then, we navigate each subjet and perform 4MomSub on it. This is a more difficult route that I did not take here.)

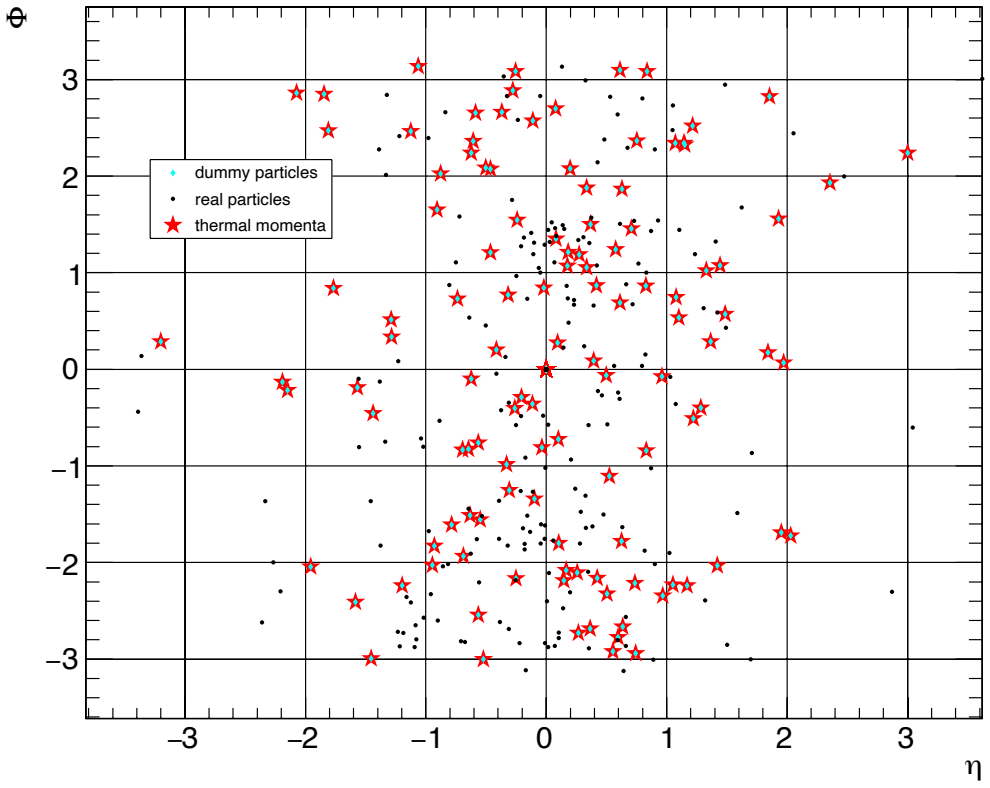

FIG. 3. When using GridSub2, we place a grid over the η-ϕ plane and assign a 4-momentum vector to each cell based on its contents. Cells have 4-momentum equal to the sum of final state particles minus the sum of thermal momenta. Cells with negative p_T are ignored. We treat those cells as particles when clustering jets using anti-k_T.

III. JET QUENCHING

A. Di-jet processes

The most common hard processes observed at RHIC energies are **di-jet** events. In di-jet processes, we generally observe two azimuthally opposite jets that are equal in p_T. As mentioned, we expect those jets to lose energies as they propagate through the medium. One observable that captures this effect is the imbalance in transverse momentum of the two jets, or "*di-jet asymmetry*", and it is defined as:

$$x_J = \frac{p_T^{sub-Lead}}{p_T^{Lead}}$$

where p_T^{Lead} and $p_T^{sub-Lead}$ are the transverse momenta of the leading and sub-leading jets respectively, meaning the ones with the highest and second-highest p_T of all jets in the event. Fig. 4 shows x_J, where the x-axis is x_J, and the y-axis the number of events for each x_J value normalized by the total number of events and bin width.

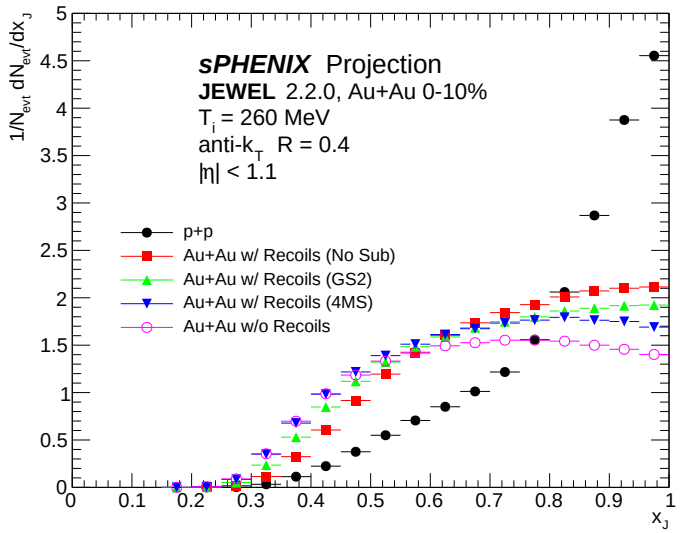

FIG. 4. Vacuum events exhibit more symmetric di-jet pairs than medium events. In medium, di-jets are asymmetric, with different effects from the two subtraction methods. Using 4MomSub (Blue) to subtract thermal background shows how hard jets are even more asymmetric without thermal contributions, while using GridSub2 (Green) has less impact on the observable.

In vacuum (p+p), the di-jet pair is imbalanced by the asymmetric emissions of the initial

partons. This causes final state partons to also have an imbalanced early stage emissions that result in a multi-jet configuration, or at least large softening of one of the jets. The distribution still peaks at $x_J = 1$.

In mediums events, additional factors play a more significant role in enhancing the asymmetry. One of those factors is the asymmetry in the path-length of the two jets. The production of a pair could take place anywhere in the medium. This means that when a di-jet pair is produced, the two jets might travel through different path-lengths. When two jets propagate through different path-lengths, they will experience different quenching effects. The longer the path-length the more softened the jet will be, and jet reconstruction algorithms do not capture the low p_T particles scattered at large angles from the jet axis. This causes the sub-leading jet to have lower p_T. Another factor, which is more important is energy loss fluctuations. Fluctuations in energy loss cause an asymmetric effect in the energy of the jets, causing this asymmetric behavior. This will be more evident when we go over path-length dependence of jet quenching in Chapter V.

Because jets lose energy as they propagate through the medium, the p_T spectrum of jets in medium is going to suffer suppression at large p_T. In detectors, soft jets with small p_T (approximately $p_T < 10$ GeV) are not even observed. In contrast, hard jets in vacuum suffer relatively weak softening and lose only a small fraction of their energy. We are more likely going to detect hard jets in p+p events than in Au+Au events. To quantify this we use the *nuclear modification factor* or R_{AA}, and it is defined as:

$$R_{AA} = \frac{1/N_{evt} dN_{AA}/dp_T}{1/N_{evt} dN_{pp}/dp_T}$$

That is, R_{AA} is the medium-to-vacuum ratio of the p_T spectra. When R_{AA} has a value less than unity, this suggests, as predicted, that we expect to see more jets in vacuum than in medium. In Fig. 5, R_{AA} is artificially high because the recoils are in the jet cone. So, some subtraction is needed. However, the different subtraction methods seem to have somewhat different impacts, so that will be something for the experimentalists to look at.

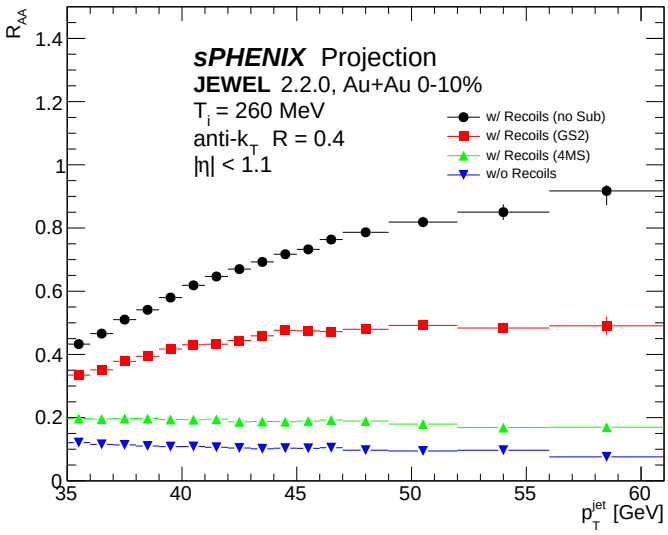

FIG. 5. Subtracting thermal background suppresses medium jets. Even though GridSub2 (red) does in fact show this suppression compared to no subtraction (black), 4MomSub (green) has more significant effect on medium jets.

B. γ-jet processes

Even though the presence of asymmetric dijet pairs could be used as evidence of the existence of QGP, energy loss in di-jet events is only relative. If a di-jet pair is produced at the center of the medium, both jets will go through the same path-length and x_J will still be unity. This does not tell us if both jets lost the same energy or if neither lost any energy. Another kind of processes that tells the story of the intrinsic energy loss is γ-jet processes. Photons only interact electromagnetically, and not strongly. Because of that, as photons travel though the medium, they have a large mean free path [10]. That is, they do not lose energy as they go through the medium. Preserving the p_T of the initial hard partons is a good way to probe the intrinsic energy loss in the leading jet. For γ-jet events, we require that the angle between the leading jet and the photon is $|\phi_\gamma - \phi_{Lead}| > 7\pi/8$. Also, jets where $|R_\gamma - R_{jet}| < 0.2$ are not considered real QCD jets, since their p_T is mostly coming from the photon.

Since a photon is expected to conserve its initial p_T, the leading jet is expected to have p_T equal to or less than that of the photon. We define the photon-jet momentum imbalance as:

$$x_{J\gamma} = \frac{p_T^{Lead}}{p_T^{\gamma}}$$

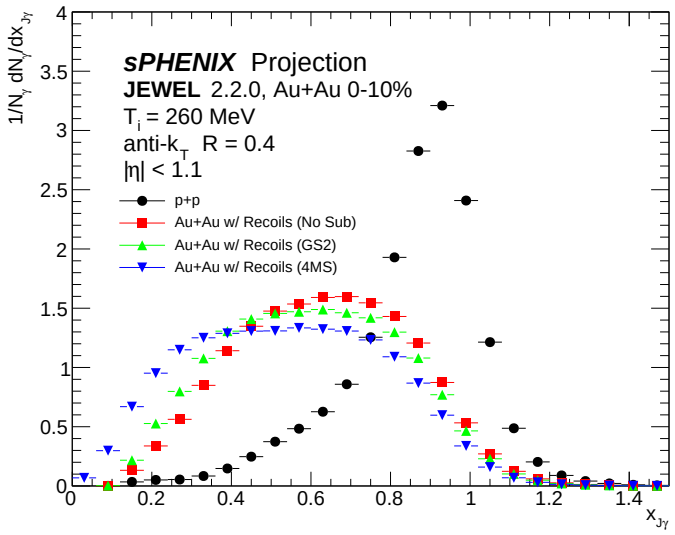

FIG. 6. The asymmetry in γ-jet events is more significant than in di-jet events (Fig. 4). This is because γ-jet events show the intrinsic energy loss the leading jet experiences.

Fig. 6 shows a more substantial gap between the asymmetry in vacuum and medium. This is because $x_{J\gamma}$ has an asymmetry even if the path-lengths of the initial particles are the same. That is, a γ-jet production at the center of the medium shows significant asymmetry as opposed to di-jet events.

Similar to R_{AA}, we use another observable I_{AA} to study the medium-to-vacuum ratio of the p_T spectra. The ratio is normalized by the number of photons. Fig. 7 shows that I_{AA} is slightly affected by the thermal contributions from the medium. This is in contrast with R_{AA} where subtraction methods have significant effects on the observable. This can only be explained by the existence of photons in the events.

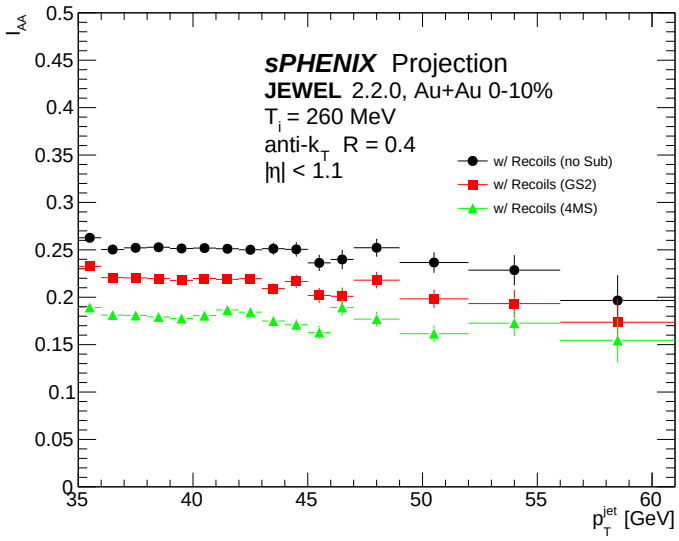

FIG. 7. The gap between subtracted jets and not subtracted jets is substantially less than what we saw in Fig. 5.

The fragmentation function D(p_T) is another observable that studies the p_T spectrum of the final state particles within the leading jet. Fig. 8 shows the medium-to-vacuum ratio of the fragmentation function. We see enhancement in low p_T particles from radiated energy and medium response. We also notice suppression in very high p_T particles.

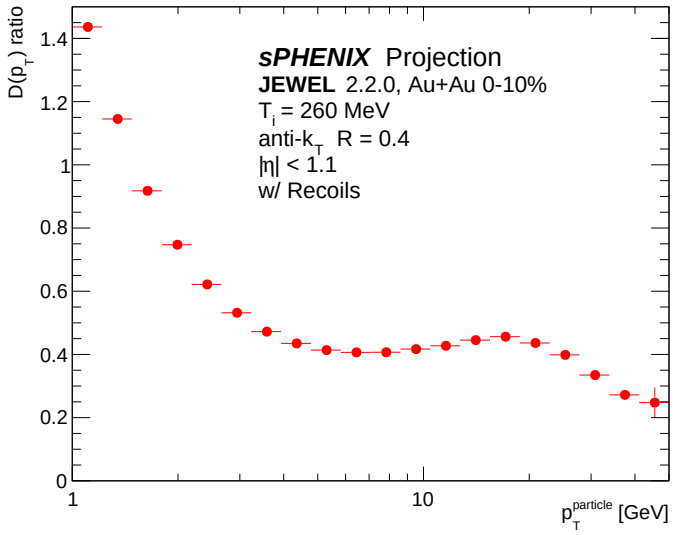

FIG. 8. For γ-jet processes in medium, leading-jets contain more soft particles than in vacuum as a result of the jet-medium interaction. Most of the high p_T particles are found in vacuum jets.

IV. JET SUB-STRUCTURE

So far, jets were used as a proxy to study the energy of hard partons produced in the initial scattering, and we have been looking at jets as indivisible entities. To fully understand jets and how they work, we need to understand their internal structure. To do that, we study jet *substructure*. When we study jet substructure, we want to find the first hard splitting of the initial hard parton, and how this affects the distribution of the final state hadrons. We use a grooming technique called *SoftDrop* to find two hard prongs (or sub-jets) within each jet [14]. Here, we are interested in how the relationship between of sub-jets changes from p+p to Au+Au events.

A. Shared Momentum Fraction z_g

To understand how SoftDrop works, we need to remember how we applied anti-k$_T$ first. When we clustered jets, we compared two particles and created a new particle-like object. We repeat this step until there are no particles left to cluster. In SoftDrop, we perform a similar idea in reverse. We de-cluster each jet into two prongs. Then, we look at the *shared momentum fraction* z_g between the two prongs defined as follows:

$$z_g = \frac{min(p_T^1, p_T^2)}{p_T^1 + p_T^2} > z_{cut}\left(\frac{\Delta R_{12}}{R_{jet}}\right)^{\beta},$$

where 1 and 2 are indices for the two prongs.
By definition, $z_g < 50\%$. We also require that $z_{cut} = 10\%$ and $\beta = 0$ (those are the values used in the first measurement of the observable by the CMS experiment at the LHC). When we require that $z_{cut} = 10\%$, we are eliminating soft prongs as candidates. Therefore, $10\% < z_g < 50\%$. If two prongs do not satisfy this requirement, we disregard the softer prong and de-cluster the harder one. We keep performing this step until we find the desired prongs.

In vacuum, jets propagate without any significant interaction. In Fig. 9, jets in vacuum tend to have hard splittings (compared to medium jets). Still, there is a high probability to have soft emissions, which comes from initial state emissions. In Au+Au events, jets interact with other partons in the medium. Therefore, they are more likely going to lose part of their energies as soft emissions. Some of those soft emissions have enough energy to

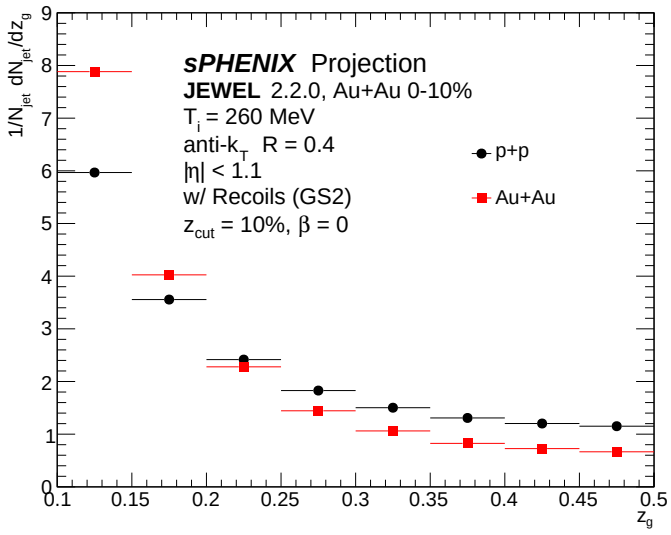

FIG. 9. The shared momentum fraction z_g is more likely going to form soft subjets in medium (red) than in vacuum (black). Conversely, in vacuum, there are more hard subjets than in medium.

form a sub-jet, but with much less energy than the hard prong. Because of this and also initial state emissions, the probability of having soft sub-jets in medium is higher than that in vacuum.

B. Splitting Angle R_g

We also look at the angle between subjets. The *splitting angle* is defined as:

$$R_g = \sqrt{(\phi_1 - \phi_2)^2 + (\eta_1 - \eta_2)^2}$$

In the previous section, we found that there are more hard splittings in vacuum than in medium. We know (see Introduction), that in the collinear limit, hard prongs tend to have small angle splittings. In contrast, the soft limit suggests that soft subjets tend to be formed at large angles from the hard ones. In Fig. 10, we see that the probability for the two subjets to have a high R_g is significantly enhanced in Au+Au.

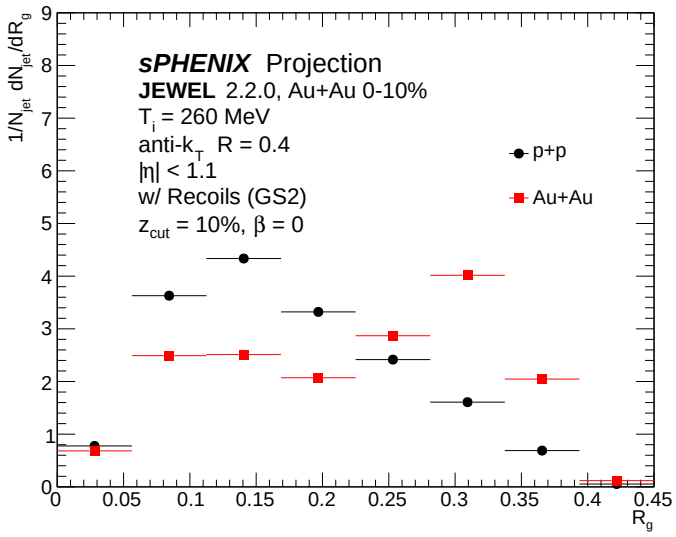

FIG. 10. The splitting angle is larger in medium (red) than in vacuum (black). This is explained by the colliner and soft limits given the behavior of the shared momentum fraction.

V. TEMPERATURE, PATH-LENGTH AND JET RADIUS

All observables that we studied so far have been set to a particular temperature (260 MeV), path-length (Au+Au) and cone size (R = 0.4). Those parameters are important to study for the next RHIC run. However, we want to test the sensitivity of jet quenching observables to those parameters. For temperature, I will use 200 MeV, 250 MeV, 300 MeV, 350 MeV and 400 MeV. For path-length, I will use Au+Au, Cu+Cu, Al+Al and O+O. For jet radius, I will use $R = 0.2, R = 0.3, R = 0.4, R = 0.6, R = 0.8$ and $R = 1.0$.

A. Temperature

The temperature of the system is expected to change the energy loss in jets in JEWEL. [1]. To test this, I use different temperatures on both x_J and R_{AA}. We note that in JEWEL, the initial temperature is actually the mean initial temperature. The default initial time is $\tau_i = 0.6\ fm$ and critical temperature is $T_c = 170$ MeV [11].

In Fig. 11, we notice that as the temperature becomes closer to the critical temperature, jet quenching becomes increasingly weaker. Di-jets tend to be more asymmetric with larger temperatures. The same goes for R_{AA} (Fig. 12), where we see enhancement in R_{AA} for jets in events with lower temperatures. However, jet quenching seems to be saturated at larger temperatures (with temperatures beyond 300 MeV), not affecting either observable significantly.

B. Path-length

In ion-ion collisions, different collision systems have different path-lengths. For example, in Au+Au collisions, there are 197 nucleons from each ion, whereas in O+O systems, there are only 16 nucleons from each ion. The length of medium that jets propagate through is different between those systems. If, as commonly accepted, the dominant effect in di-jet asymmetry is the difference in path-lengths, then we expect substantial changes in x_J as we go from smaller to larger systems.

However, as we see in Figure 13, di-jet asymmetry is hardly affected when we change the path-length. This suggests that, as mentioned in chapter II, di-jet asymmetry is not

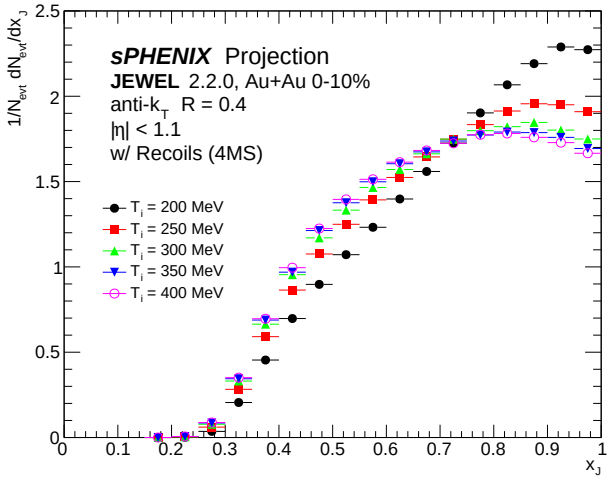

FIG. 11. x_J becomes sharper with lower T_i. It becomes insensitive to changes in T_i when T_i is large

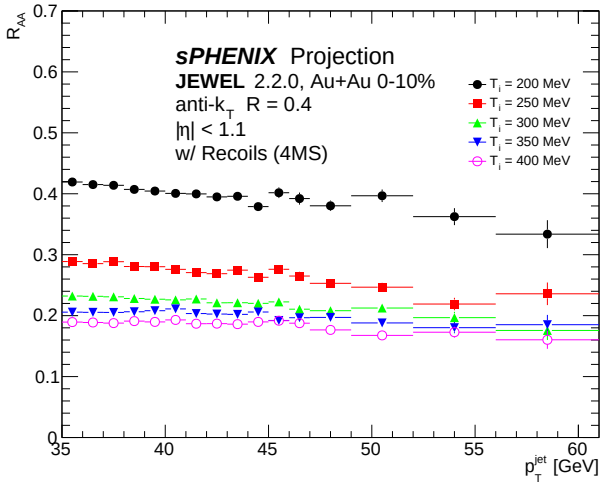

FIG. 12. R_{AA} is more sensitive to changes in the temperature when it is closer the critical temperature.

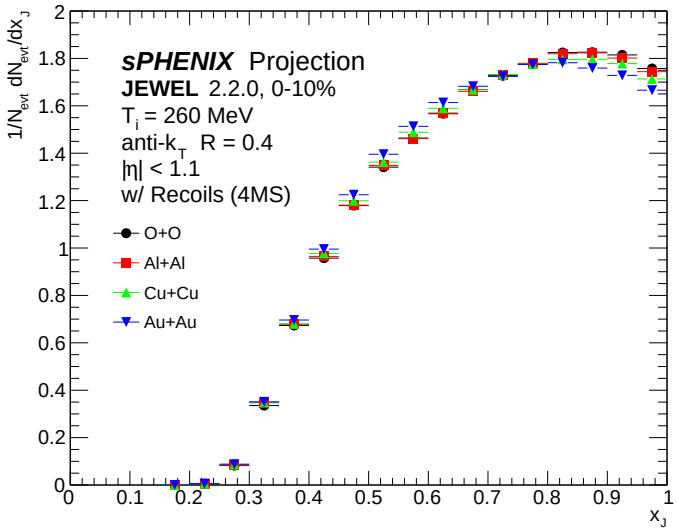

FIG. 13. x_J is independent of the path-length of the system. This is because the di-jet asymmetry in JEWEL is driven by the fluctuations in the energy loss.

primarily driven by differences in path-length, at least in the JEWEL model of jet-medium interactions. The main cause of the asymmetry is the fluctuations in the energy loss [12].

In Figure 14, we see that the change in R_{AA} between different systems supports the idea

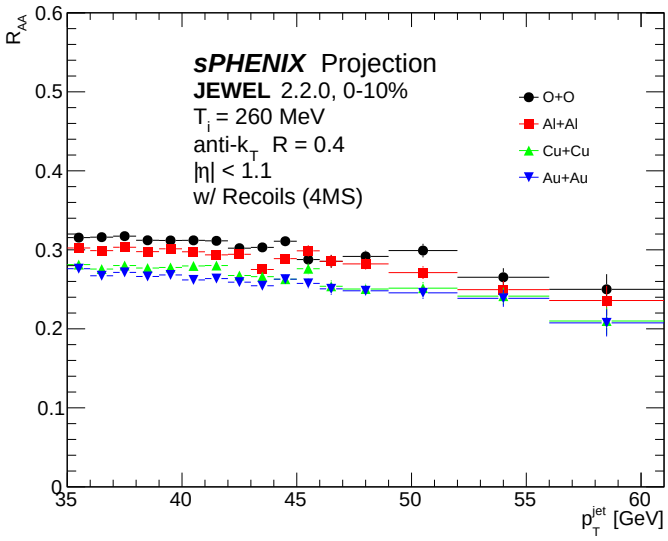

FIG. 14. Different path-lengths exhibit a very small change in R_{AA} as we go to larger systems.

that fluctuations are the driving factor for di-jet asymmetry. This is because the change in R_{AA} means that energy loss does change between those systems and yet the di-jet asymmetry is unchanged.

C. Jet Radius

Studies suggest that most of the lost energy in heavy-ion collisions can be found as soft emissions distributed over the two hemispheres that contain each jet (or a photon and a jet in γ-jet events) [15]. That is, smaller jet radii contain information about only the hard clusters in the η-ϕ plane. If we include more particles when clustering jets (i.e. use larger jet radii), we expect to recover most of the lost energy.

In Figure 15, increasing the radius of the leading jet in a γ-jet event makes the system recover its symmetry. This is because we are including more soft particles in the event. When $R = 1$ (Fig. 16), the distribution looks similar to that of vacuum events. From Figure 17, when using larger jet radii, I_{AA} becomes larger recovering the lost energy. At large p_T, I_{AA} becomes close to unity. Smaller jet radii (0.2,0.3,0.4) have almost the same I_{AA}. This suggests that the hard parts of the jets are actually small compared to the jet size that we have been using ($R = 0.4$). There is a gap between the hard parts of jets and the point where we start recovering soft emissions that compensate the energy loss.

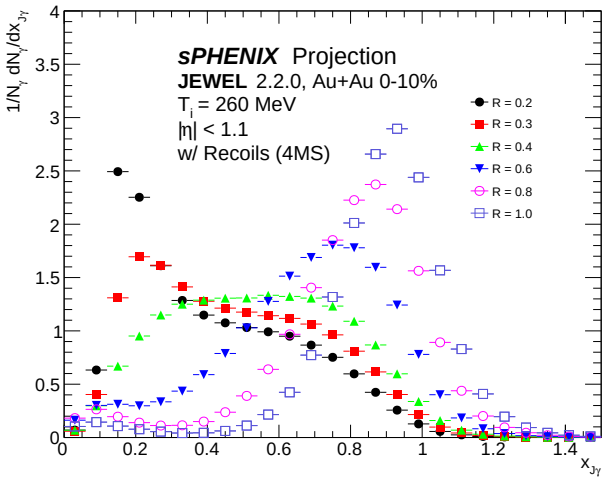

FIG. 15. Increasing the radius of the leading jet recovers most of the lost energy in the event.

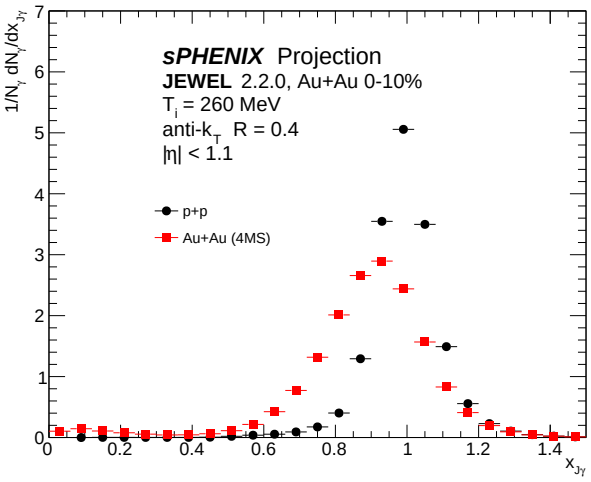

FIG. 16. In the case of $R = 1$, the asymmetry in γ-jet processes becomes closer to the vacuum case.

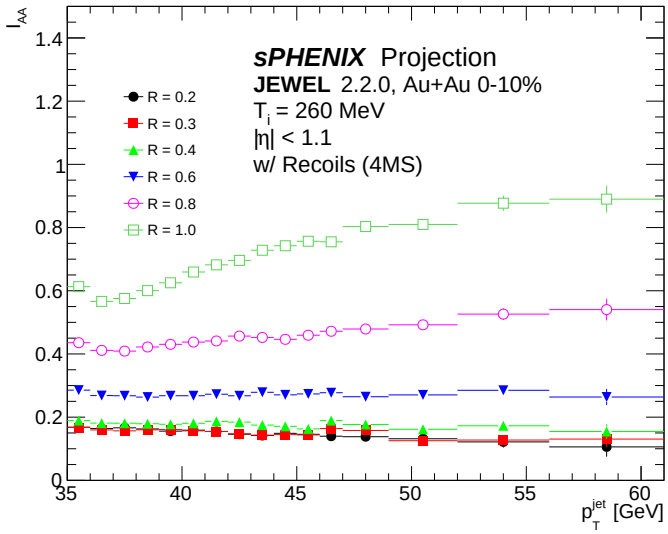

FIG. 17. I_{AA} for different jet radii shows how we can recover energy loss in ion-ion collisions. In the case of high p_T and $R = 1$, I_{AA} becomes closer to unity.

In Fig. 18, we see the contents of the leading jet with different radii. Since when we increase the radius of the leading jet, we are only recovering soft emissions, the high p_T contents of jets with different radii is the same. The only difference is how many low p_T particles they contain.

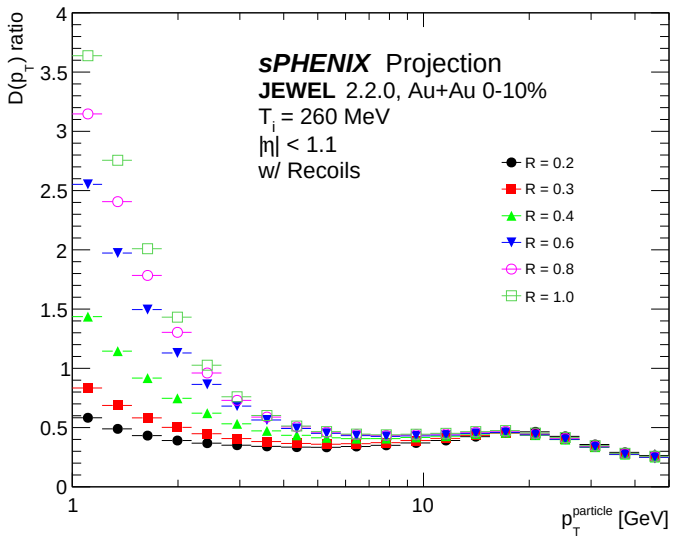

FIG. 18. When the radius of the leading jets becomes larger, the soft contents of those jets increase. The large number of low p_T particles outside the jet is a result of the medium-jet interaction.

VI. CONCLUSION

Using JEWEL 2.2.0, I made predictions for different jet quenching obeservables. For the analysis, I used both di-jet and γ-jet processes. In both cases, we compared the p_T asymmetry in the event by studying x_J and $x_{J\gamma}$ respectively. We also studied the behavior of the jet p_T spectrum in medium events compared to vacuum events.

For jet sub-structure, we made predictions for the splitting function and the splitting angle using SoftDrop. We found that in medium, we expect more soft sub-jets and larger splitting angles compared to vacuum.

We also tested jet quenching observables sensitivity to some parameters. We found that temperature dependence becomes more important at temperatures closer to the T_c. At larger temperatures, the observables become insensitive to the change in T_i. For path-length, di-jet asymmetry was independent of the collision system used. There was no change in the di-jet asymmetry between different systems. This is because in JEWEL, di-jet asymmetry is driven by energy loss fluctuations and not differences in path-length. Lastly, using different jet radii, we were able to recover most of the lost energy of the leading jet in γ-jet events.

The upcoming sPHENIX detector and the upgrades to the STAR detector are full of exciting new physics. One of the best tools to study the physics at RHIC energies is JEWEL 2.2.0. This is particularly true for the sPHENIX detector where we will see the first full jet reconstruction where all particles are measured at RHIC. For those reasons, JEWEL can be useful in studying jet quenching for the detector. The sPHENIX will start taking data in 2023, and we look forward to studying those data in the next RHIC runs.

[1] Korinna Zapp, Gunnar Ingelman, Johan Rathsman, Johanna Stachel, and Urs Achim Wiedemann, "A monte carlo model for "jet quenching"," The European Physical Journal C **60** (2009), 10.1140/epjc/s10052-009-0941-2.

[2] Korinna C. Zapp, Frank Krauss, and Urs A. Wiedemann, "A perturbative framework for jet quenching," JHEP **03**, 080 (2013), arXiv:1212.1599 [hep-ph].

[3] A. Adare *et al.* (PHENIX), "An Upgrade Proposal from the PHENIX Collaboration," (2015), arXiv:1501.06197 [nucl-ex].

[4] Andrew Larkoski, *Elementary particle physics: an intuitive introduction* (Cambridge University Press, Cambridge, 2019).

[5] Wikipedia contributors, "Standard model — Wikipedia, the free encyclopedia," (2021), [Online; accessed February-2021].

[6] Edward Shuryak, *Quantum many-body physics in a nutshell*, In a nutshell (Princeton University Press, Princeton, NJ, 2019).

[7] Christopher C Tully, *Elementary particle physics in a nutshell* (Princeton Univ. Press, Princeton, NJ, 2011).

[8] Matteo Cacciari, Gavin P. Salam, and Gregory Soyez, "The anti-k_t jet clustering algorithm," JHEP **04**, 063 (2008), arXiv:0802.1189 [hep-ph].

[9] Simone Marzani, Gregory Soyez, and Michael Spannowsky, "Looking inside jets," Lecture Notes in Physics (2019), 10.1007/978-3-030-15709-8.

[10] Cheuk-Yin Wong, *Introduction to high-energy heavy-ion collisions* (World Scientific, Singapore, 1994) erratum.

[11] Korinna C. Zapp, "JEWEL 2.0.0: directions for use," Eur. Phys. J. C **74**, 2762 (2014), arXiv:1311.0048 [hep-ph].

[12] José Guilherme Milhano and Korinna Christine Zapp, "Origins of the di-jet asymmetry in heavy ion collisions," Eur. Phys. J. C **76**, 288 (2016), arXiv:1512.08107 [hep-ph].

[13] Raghav Kunnawalkam Elayavalli and Korinna Christine Zapp, "Medium response in JEWEL and its impact on jet shape observables in heavy ion collisions," JHEP **07**, 141 (2017), arXiv:1707.01539 [hep-ph].

[14] Andrew J. Larkoski, Simone Marzani, Gregory Soyez, and Jesse Thaler, "Soft Drop," JHEP

05, 146 (2014), arXiv:1402.2657 [hep-ph].

[15] Vardan Khachatryan *et al.* (CMS), "Measurement of transverse momentum relative to dijet systems in PbPb and pp collisions at $\sqrt{s_{\mathrm{NN}}} = 2.76$ TeV," JHEP **01**, 006 (2016), arXiv:1509.09029 [nucl-ex].